Appl. Phys. B 48, 427–435 (1989)

Applied Physics B Photophysics and Laser Chemistry



# First-Stage Enrichment in $CO_2$-Laser-Induced $^{13}C$ Separation by a Two-Stage IRMPD Process: IRMPD of $CHClF_2/Br_2$ Mixtures

**S. Arai[1], K. Sugita[2], P. Ma[2]*, Y. Ishikawa[2], H. Kaetsu[2], and S. Isomura[2]**

[1] Kyoto Institute of Technology, Matsugasaki, Sakyo-ku, Kyoto 606, Japan
[2] The Institute of Physical and Chemical Research, Wako-shi, Saitama 351-01, Japan

Received 17 October 1988/Accepted 3 November 1988

**Abstract.** We have been studying the practical $CO_2$-laser-induced $^{13}C$ separation by a two-stage IRMPD process. The IRMPD of natural $CHClF_2$ in the presence of $Br_2$ mainly produced $CBr_2F_2$, which was found to be highly enriched with $^{13}C$. The yield and $^{13}C$-atom fraction of $CBr_2F_2$ were examined as functions of pulse number, laser line, laser fluence, total pressure, and $Br_2$ pressure using a $CO_2$ TEA laser with an output less than 1 J pulse$^{-1}$ in order to optimize experimental conditions for $^{13}C$ separation. For example, we obtained $CBr_2F_2$ at a $^{13}C$ concentration of 55% in the irradiation of the mixture of 100-Torr $CHClF_2$ and 10-Torr $Br_2$ with the laser radiation at a wavenumber of 1045.02 cm$^{-1}$ and at a fluence of 3.4 J cm$^{-2}$. The mechanism for the IRMPD is discussed on the basis of observed results. Using 8-J pulses, we were able to obtain $1.9 \times 10^{-4}$ g of $^{13}C$-enriched $CBr_2F_2$ ($^{13}C$-atom fraction, 47%) per pulse under selected conditions. It is possible to produce 90% or higher $^{13}C$ by the second-stage IRMPD of the $CBr_2F_2$ in the presence of oxygen.

**PACS:** 82.50, 33

Since the discovery of isotopically selective photodecomposition of molecules in intense IR fields, infrared multiple-photon decomposition (IRMPD) is expected to be applicable to practical isotope separation in a near future [1]. Of a number of isotopes from $^2H$ to $^{235}U$, $^{13}C$ separation has been most extensively investigated in IRMPD [2–9]. Most of previous studies have been succinctly reviewed in the introductory section of the paper by Outhouse et al. [7].

Although remarkably large selectivities have been achieved in IRMPD of fluorocarbons such as $CF_3X$ ($X$ = Cl, Br, or I) [10, 11] and $CHClF_2$ [3, 9], it is very difficult to obtain practical amounts of $^{13}C$ at a sufficiently high purity in a single-stage IRMPD process. A number of previous studies have shown that 90% or higher $^{13}C$ is only obtainable with a great sacrifice of its yield. In a few studies, high enrichment of $^{13}C$ was attained by eliminating extensively $^{12}C$-bearing molecules from natural $CF_3I$ [12, 13]. However, the process cannot be efficient, because of the natural abundance ratio of $^{12}C$ to $^{13}C$, i.e., 98.9%: 1.1%. There seems to be a general agreement that the practical enrichment of $^{13}C$ by IRMPD requires a two-stage process.

In previous papers, we have proposed several chemical systems suitable for a two-stage IRMPD process, wherein the product in the first-stage selective IRMPD was at once used as the working substance in the second-stage IRMPD for further enrichment [14–16]. For example, the IRMPD of $CHClF_2/Br_2$ mixtures produced $CBr_2F_2$ at a high yield, if the $^{13}C$-atom fraction was suppressed in the range of 30–50%. The second-stage IRMPD of the $CBr_2F_2$ in the presence of $O_2$ gave rise to $CF_2O$, which was highly enriched with $^{13}C$ [16]. The subsequent hydrolysis of the $CF_2O$ was found to give $^{13}C$-enriched $CO_2$ as a final product, which was an useful material for chemical synthesis of $^{13}C$-labeled organic compounds. This

* Present address: Quinghai Institute of Saline Lake, Academia Sinica, Xining, People's Republic of China

process could be one of the most promising approaches to practical laser $^{13}C$ separation. In the present study we examined the first-stage enrichment as functions of several experimental parameters to establish optimal conditions for separation. In addition, the mechanism for the IRMPD will be discussed in light of observed results.

## 1. Experimental

The apparatus and procedures are almost the same as those described previously [16]. The beams from a Lumonics 103 $CO_2$ TEA laser were focused by a $BaF_2$ lens with a focal length of 170 cm after truncation by a circular iris (diameter 2.0 cm). A short irradiation cell (length 10 cm; inner diameter 2.0 cm) equipped with NaCl windows at both ends was placed in parallel with the beam and in a vicinity of the focal point. In this optical geometry the fluence inside an illuminated zone can be regarded as almost homogeneous. The cell volume was 48.9 $cm^3$. The fluence was, if necessary, varied by inserting one or more polyethylene films into the beam in front of the lens. The laser was operated at a repetition rate of 0.7 Hz using a mixture of He and $CO_2$ as a lasing medium. The resulting pulse had a triangle profile (80-ns FWHM) without a tail. Products were analyzed on a GC-MS (GC column, 6 m × 3 mm Gaskuropack-55; column temperature 150 °C).

A Lumonics 822 $CO_2$ TEA laser, which provides 10-J pulses at a maximum output, was employed for preliminary large-scale photolysis. The lasing medium was a mixture of He, $CO_2$, $N_2$, and $H_2$. The pulse consisted of an initial spike (200 ns FWHM) and a long tail containing 30% of the total energy. The output was adjusted to 8 J per pulse. The beams focused by a lens (focal length 210 cm) were introduced into a 4-m long irradiation cell with NaCl windows; the fluence distribution was inhomogeneous along the beam. In an empty cell the fluence was found to be 7.9 J $cm^{-2}$ at a beam waist. Sample gases were continuously circulated during irradiation by means of a small pump. The cell volume including the pump was $5.0 \times 10^3$ $cm^3$.

## 2. Results

The detailed infrared spectrum of $CHClF_2$ and the IR band assignments have been reported in the paper by McLaughlin et al., where $CHClF_2$ was dissolved into liquid argon at 110 K [17]. The compound has an intense band at 1100 $cm^{-1}$ due to a symmetric $^{12}C$–F stretching vibration mode, and its isotope shift by $^{13}C$ is 24 $cm^{-1}$. The $CO_2$ laser radiation in the 9*P* and 9*R* branches pumps $CHClF_2$ molecules to high vibrational states via multiple-photon absorption. The products in the IRMPD of neat $CHClF_2$ have been found to be $C_2F_4$ and HCl [18].

Upon adding $Br_2$ to $CHClF_2$, $C_2F_4$ is replaced by new products $CBr_2F_2$ and $C_2Br_2F_4$; the yield of the former product is much larger than that of the latter. Figure 1 shows their yields as a function of pulse number, where $CBr_2F_2 = {}^{12}CBr_2F_2 + {}^{13}CBr_2F_2$ and $C_2Br_2F_4 = {}^{12,12}C_2Br_2F_4 + {}^{12,13}C_2Br_2F_4 + {}^{13,13}C_2Br_2F_4$. In the yields, the sum of $CBr_2F_2$, $C_2Br_2F_4$, and unconsumed $CHClF_2$ was taken as 100%. In the experiment the mixtures of 10-Torr $CHClF_2$ and 1-Torr $Br_2$ were irradiated with the 9*P*(22) line at 1045.02 $cm^{-1}$. The fluence was about 3.1 $cm^{-2}$. The yield of $CBr_2F_2$ increases linearly with increasing pulse number, while that of $C_2Br_2F_4$ increases concavely. Therefore, the ratio between the two yields, $[CBr_2F_2]/[C_2Br_2F_4]$ apparently increases with increasing pulse number, although the data scatters widely as shown in Fig. 2. In Fig. 3, the $^{13}C$-atom fractions in $CBr_2F_2$ and $C_2Br_2F_4$ are plotted against pulse number. Both $^{13}C$-atom fractions have almost the same value, i.e., about 34 at the beginning of irradiation. However, the fraction in $CBr_2F_2$ decreases and that in $C_2Br_2F_4$ increases with an increase in pulse number. The decrease in $CBr_2F_2$ is probably due to diminishing concentration of a $^{13}C$-bearing molecule in $CHClF_2$. On the other hand, the increase in $C_2Br_2F_4$ may arise from the secondary photolysis of $C_2Br_2F_4$, as explained later in detail.

To clarify the pulse number effects on the IRMPD further, $^{12}C$- and $^{13}C$-production yields in $CBr_2F_2$ and $C_2Br_2F_4$ as well as corresponding yields per pulse are plotted against pulse number in Figs. 4 and 5. Their definitions are as follows:

$^{12}C$-production yield in $CBr_2F_2$,

$$^{12}Y(CBr_2F_2) = \frac{\text{amount of } ^{12}C \text{ in } CBr_2F_2}{\text{initial amount of } ^{12}C \text{ in } CHClF_2}$$

$^{13}C$-production yield in $CBr_2F_2$,

$$^{13}Y(CBr_2F_2) = \frac{\text{amount of } ^{13}C \text{ in } CBr_2F_2}{\text{initial amount of } ^{13}C \text{ in } CHClF_2}.$$

The initial amounts of $^{12}C$ and $^{13}C$ in $CHClF_2$ are equal to 98.9 and 1.1% of $CHClF_2$ before irradiation, respectively.

$^{12}C$-production yield per pulse in $CBr_2F_2$

$$^{12}y(CBr_2F_2) = {}^{12}Y(CBr_2F_2)/\text{pulse number}$$

$^{13}C$-production yield per pulse in $CBr_2F_2$

$$^{13}y(CBr_2F_2) = {}^{13}Y(CBr_2F_2)/\text{pulse number}$$

$^{12}Y(C_2Br_2F_4)$, $^{13}Y(C_2Br_2F_4)$, $^{12}y(C_2Br_2F_4)$, and $^{13}y(C_2Br_2F_4)$ are defined similarly to those for

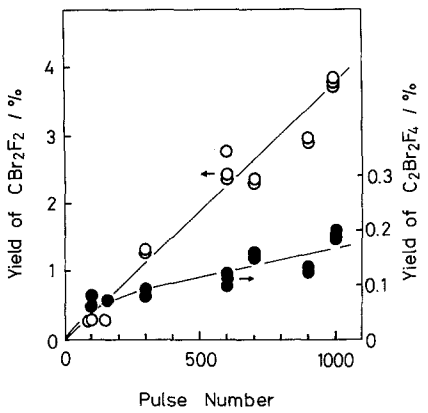


**Fig. 1.** Yields of $CBr_2F_2$ and $C_2Br_2F_4$ vs. pulse number. $CHClF_2$, 10 Torr; $Br_2$, 1 Torr; laser line, $9P(22)$ at 1045.02 $cm^{-1}$; fluence, 3.0–3.2 J $cm^{-2}$

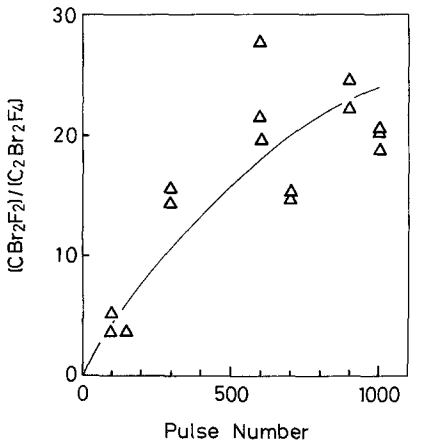


**Fig. 2.** Ratio of $[CBr_2F_2]$ to $[C_2Br_2F_4]$ vs. pulse number. Irradiation conditions, see the caption of Fig. 1

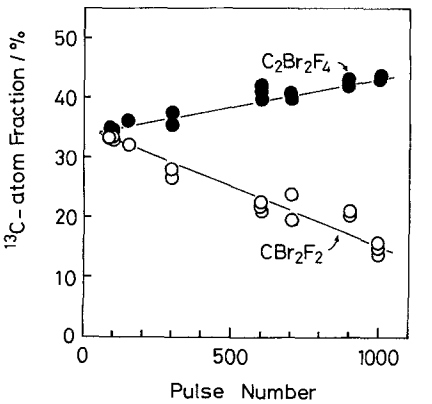


**Fig. 3.** $^{13}C$-atom fractions in $CBr_2F_2$ and $C_2Br_2F_4$ vs. pulse number. Irradiation conditions, see the caption of Fig. 1

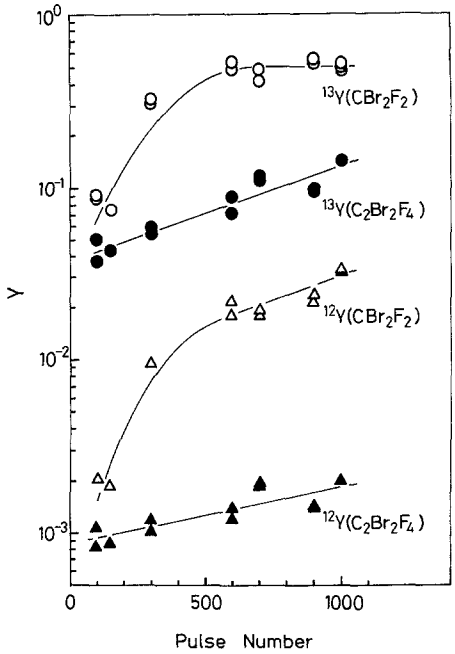


**Fig. 4.** Carbon isotope production yields in $CBr_2F_2$ and $C_2Br_2F_4$ vs. pulse number. $^{12}Y(CBr_2F_2)$, $^{13}Y(CBr_2F_2)$, $^{12}Y(C_2Br_2F_4)$, and $^{13}Y(C_2Br_2F_4)$, see text. Irradiation conditions, see the caption of Fig. 1

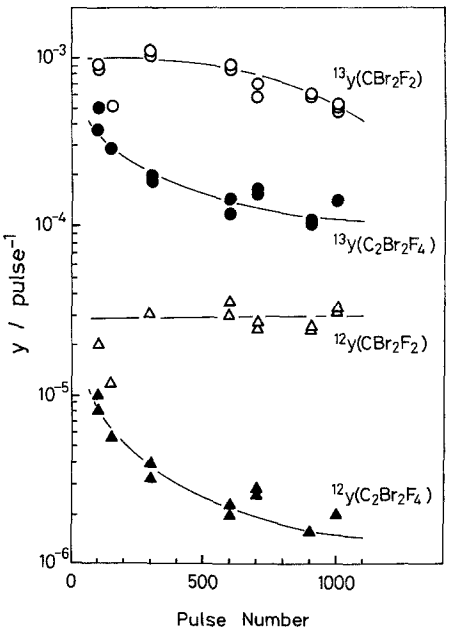


**Fig. 5.** Production yields per pulse vs. pulse number. $^{12}y(CBr_2F_2)$, $^{13}y(CBr_2F_2)$, $^{12}y(C_2Br_2F_4)$, and $^{13}y(C_2Br_2F_4)$, see text. Irradiation conditions, see the caption of Fig. 1

$CBr_2F_2$. In Fig. 4, $^{13}Y(CBr_2F_2)$ reaches a plateau value of 0.5 at 600 shots and the further irradiation does not result in an essential production of $^{13}CBr_2F_2$. However, $^{12}Y(CBr_2F_2)$ appears to increase after 600 shots; therefore, the $^{13}C$-atom fraction in $CBr_2F_2$ decreases at high pulse numbers. $^{13}y(CBr_2F_2)$ decreases with increasing pulse number above 600 shots, whereas $^{12}y(CBr_2F_2)$ is approximately flat in the region examined, as shown in Fig. 5. On the other hand, both $^{12}y(C_2Br_2F_4)$ and $^{13}y(C_2Br_2F_4)$ show

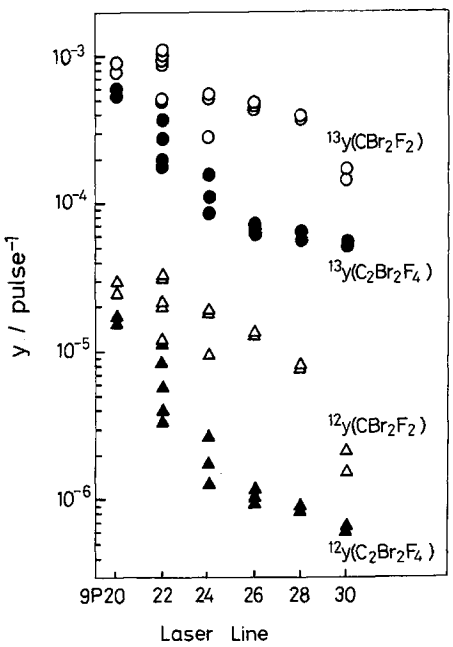


**Fig. 6.** $^{12}y(CBr_2F_2)$, $^{13}y(CBr_2F_2)$, $^{12}y(C_2Br_2F_4)$, and $^{13}y(C_2Br_2F_4)$ vs. laser line. $CHClF_2$, 10 Torr; $Br_2$, 1 Torr. Fluence and pulse number: $9P(20)$, 3.2 J cm$^{-2}$ and 100 shot; $9P(22)$, 3.1–3.3 J cm$^{-2}$ and 100–300 shots; $9P(24)$, 2.4–2.9 J cm$^{-2}$ and 200–1000 shots; $9P(26)$, 3.1 J cm$^{-2}$ and 1000 shots; $9P(28)$, 2.8 J cm$^{-2}$ and 1000 shots; $9P(30)$, 2.3 J cm$^{-2}$ and 1000 shots

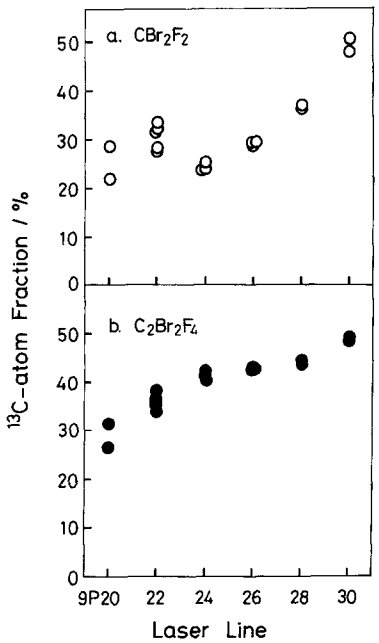


**Fig. 7.** $^{13}$C-atom fractions in $CBr_2F_2$ and $C_2Br_2F_4$ vs. laser line. Irradiation conditions, see the caption of Fig. 6

rapid decreases even at the beginning of the irradiation. This fact suggests the secondary photochemical decomposition of the compound.

Figures 6 and 7 present laser line effects on $^{12}$C- and $^{13}$C-production yields and $^{13}$C-atom fractions in

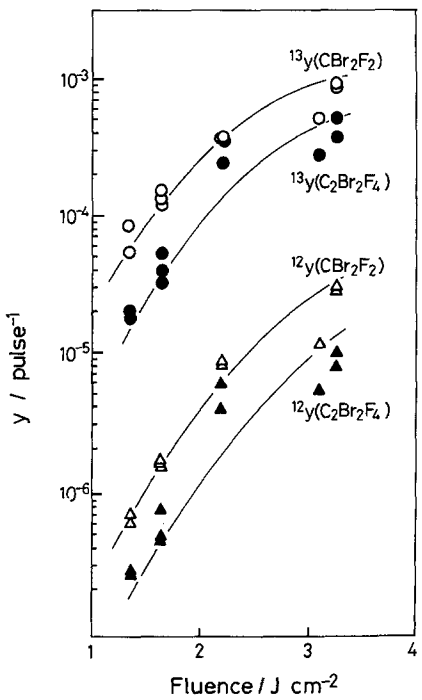


**Fig. 8.** $^{12}y(CBr_2F_2)$, $^{13}y(CBr_2F_2)$, $^{12}y(C_2Br_2F_4)$, and $^{13}y(C_2Br_2F_4)$ vs. fluence. $CHClF_2$, 10 Torr; $Br_2$, 1 Torr; laser line, $9P(22)$. Pulse number: 1000 shots at 1.10 J cm$^{-2}$; 1000 shots at 1.35 J cm$^{-2}$; 1000 shots at 1.65 J cm$^{-2}$; 180 shots at 2.21 J cm$^{-2}$; 150 shots at 3.10 J cm$^{-2}$; 100 shots at 3.26 J cm$^{-2}$

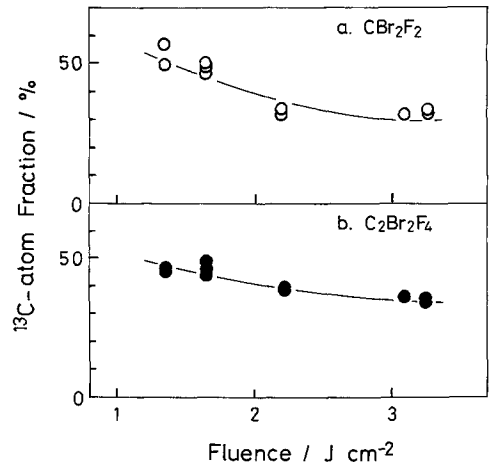


**Fig. 9.** $^{13}$C-atom fractions in $CBr_2F_2$ (a) and $C_2Br_2F_4$ (b) vs. fluence. Irradiation conditions, see the caption of Fig. 8

$CBr_2F_2$ and $C_2Br_2F_4$, respectively, on the IRMPD of mixtures of 10-Torr $CHClF_2$ and 1-Torr $Br_2$. Large scatters in the figures may be caused by the differences in experimental parameters such as fluence and pulse number among the runs. Roughly speaking, $^{12}y(CBr_2F_2)$ and $^{13}y(CBr_2F_2)$ decrease, and the $^{13}$C-atom fraction in $CBr_2F_2$ increases, as the laser line is changed in the order from $9P(20)$ (1046.85 cm$^{-1}$) to $9P(30)$ (1037.44 cm$^{-1}$). Although the final products are different from each other between the cases with and

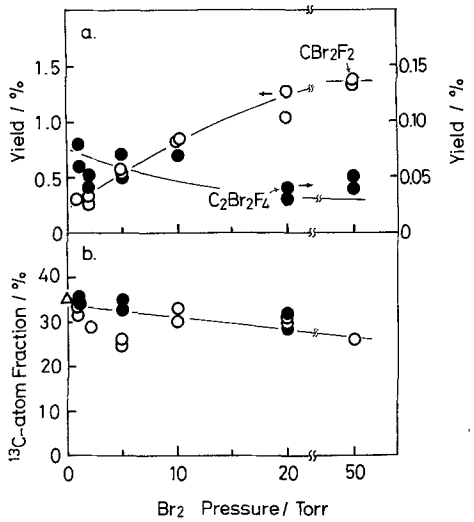


**Fig. 10.** Yields of $CBr_2F_2$ and $C_2Br_2F_4$ vs. $Br_2$ pressure (a), and $^{13}C$-atom fractions in $CBr_2F_2$ and $C_2Br_2F_4$ vs. $Br_2$ pressure (b). $CHClF_2$, 10 Torr; laser line, $9P(22)$; pulse number, 100 shots; fluence, about 3.4 J $cm^{-2}$. The $^{13}C$-atom fraction in $C_2F_4(\Delta)$ produced with the photolysis of neat $CHClF_2$ (10 Torr) is also shown in Fig. 10b

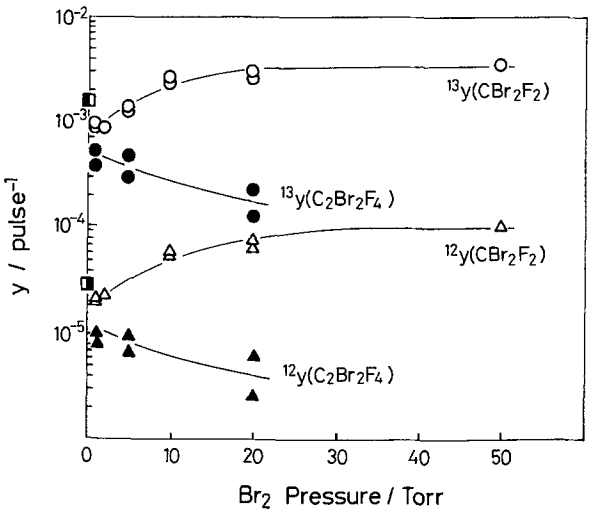


**Fig. 11.** $^{12}y(CBr_2F_2)$, $^{13}y(CBr_2F_2)$, $^{12}y(C_2Br_2F_4)$, and $^{13}y(C_2Br_2F_4)$ vs. $Br_2$ pressure. Irradiation conditions, see the caption of Fig. 10. ◧ and ◨ are $^{13}y(C_2F_4)$ and $^{12}y(C_2F_4)$, respectively, for near $CHClF_2$

without $Br_2$, the initial photochemical step is the decomposition of a resonant molecule $CHClF_2$ in an intense laser field. Therefore, the product yields and product selectivities should depend on the initial decomposition. The tendencies in Figs. 6 and 7 are consistent with those observed for the IRMPD of neat $CHClF_2$ [3].

Figures 8 and 9 show fluence effects on yields and $^{13}C$-atom fractions in $CBr_2F_2$ and $C_2Br_2F_4$, where the pressures of $CHClF_2$ and $Br_2$ are 10 and 1 Torr, respectively, and the laser line is $9P(22)$ at 1045.02 $cm^{-1}$. As observed for IRMPD in general, the

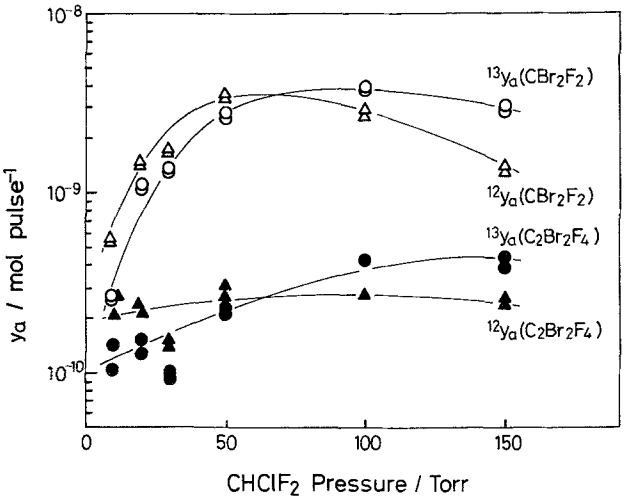


**Fig. 12.** Absolute yields per pulse vs. $CHClF_2$ pressure. $^{12}y_a(CBr_2F_2)$, $^{13}y_a(CBr_2F_2)$, $^{12}y_a(C_2Br_2F_4)$, and $^{13}y_a(C_2Br_2F_2)$, see text. $Br_2$, 10% of $CHClF_2$; laser line, $9P(22)$; pulse number, 100 shots; fluence, ca. 3.5 J $cm^{-2}$

production yields increase and the selectivities in products decrease with an increase in laser fluence. When a fluence was higher than 10 J $cm^{-2}$, we found a large amount of $CBrClF_2$ in addition to $CBr_2F_2$ and $C_2Br_2F_4$. The formation can be explained by a thermal chain mechanism, as described later.

Figures 10 and 11 shows the $Br_2$ pressure effects on the yields, $^{13}C$-atom fractions, and production yields in $CBr_2F_2$ and $C_2Br_2F_4$. The $CHClF_2$ pressure and fluence were kept constant at 10 Torr and ca. 3.4 J $cm^{-2}$, respectively. The irradiation wavenumber was $9P(22)$ (1045.02 $cm^{-1}$). Since all mixtures were irradiated with 100 pulses, $^{12}y$ or $^{13}y$ equals $^{12}Y/100$ or $^{13}Y/100$ in Fig. 11. The total yield of $CBr_2F_2$, i.e., $^{12}CBr_2F_2 + {}^{13}CBr_2F_2$ reaches a plateau value above 20-Torr $Br_2$, while the total yield of $C_2Br_2F_4$ decreases with increasing $Br_2$, as shown in Fig. 10a. The $^{13}C$-atom fractions in both $CBr_2F_2$ and $C_2Br_2F_4$ show slight decreases with increasing $Br_2$ in Fig. 10b. It is worth mentioning that the extrapolated value of the atom fraction vs. $Br_2$ pressure curve to the ordinate agrees closely with the atom fraction observed for the $C_2F_4$ produced from the IRMPD of neat $CHClF_2$ under the same irradiation conditions. $^{12}y(CBr_2F_2)$ and $^{13}y(CBr_2F_2)$ increase initially with an increase in $Br_2$, while both $^{12}y(C_2Br_2F_4)$ and $^{13}y(C_2Br_2F_4)$ appear to decrease with increasing $Br_2$.

Effects of total pressure on absolute production yields are shown in Fig. 12, where the absolute production yield of $^{12}CBr_2F_2$, $^{12}y_a(CBr_2F_2)$ is defined as the amount of $^{12}C$ in $CBr_2F_2$ (in a mole unit) divided by pulse number. The other absolute yields $^{13}y_a(CBr_2F_2)$,

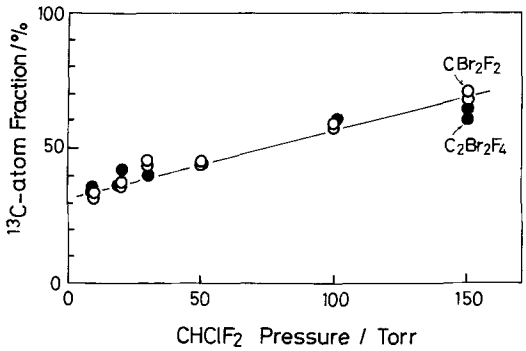


**Fig. 13.** $^{13}$C-atom fractions in $CBr_2F_2$ and $C_2Br_2F_4$ vs. $CHClF_2$ pressure. Irradiation conditions, see the caption of Fig. 12

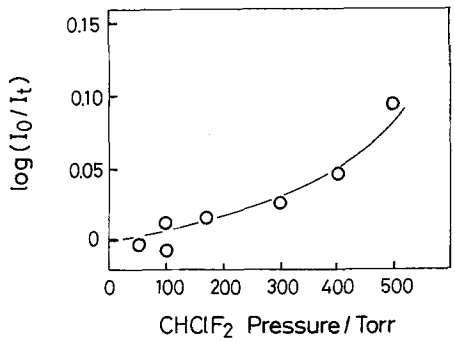


**Fig. 14.** Logarithmic plots of $I_0/I_t$ vs. $CHClF_2$ pressure. $I_0$ and $I_t$ are the laser pulse energies passing through empty and filled cells, respectively. The optical path length of a cell is 10 cm. Laser line, 9*P*(22); fluence, 3.0–3.3 J cm$^{-2}$

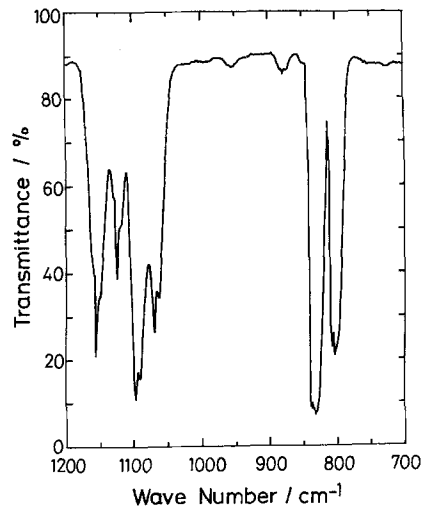


**Fig. 15.** The infrared absorption spectrum of $^{13}$C-enriched $CBr_2F_2$. The $CBr_2F_2$ was produced from the IRMPD of the mixture of 100 Torr $CHClF_2$ and 45 Torr $Br_2$. Laser line, 9*P*(22); fluence at a beam waist, about 6.3 J cm$^{-2}$

$^{12}y_a(C_2Br_2F_4)$, and $^{13}y_a(C_2Br_2F_4)$ are defined similarly to $^{12}y_a(CBr_2F_2)$. The ratios of $[CHClF_2]$ to $[Br_2]$ are 10 in all mixtures. The detailed irradiation conditions are described in the figure caption. Both $^{12}y_a(CBr_2F_2)$ and $^{13}y_a(CBr_2F_2)$ initially increase and, after passing maxima, gradually decrease with increasing $CHClF_2$ pressure, as shown in Fig. 12. The maxima seem to be located around 100 Torr. On the other hand, $^{13}y_a(C_2Br_2F_4)$ increases by a factor of about 4 with an increase in the pressure and $^{12}y_a(C_2Br_2F_4)$ is flat in the region examined. The $^{13}$C-atom fractions in $CBr_2F_2$ and $C_2Br_2F_4$ clearly increase with increasing pressure, as shown in Fig. 13. Such an increase in selectivity with increasing pressure has been also observed for the IRMPD of neat $CHClF_2$ [3].

$CHClF_2$ does not absorb appreciably the laser radiation under the present irradiation conditions, unless its pressure exceeds 100 Torr. A plot of $\log(I_0/I_t)$ vs. $CHClF_2$ pressure is given in Fig. 14, where $I_0$ and $I_t$ correspond to the light intensities passing through the 10-cm length cell without $CHClF_2$ and with $CHClF_2$ at a certain pressure, respectively. The absorption cross section seems to become larger at higher pressure, deviating from the Lambert-Beer law. One possible explanation is as follows. Laser radiation is considered to pump resonating molecules at a particular rotational state. The observed increase in absorption may be caused by collision-induced rotational relaxation which supplies resonating molecules at the state. Another possible explanation is that the secondary absorption of laser radiation by the "hot" molecules of non-resonating $^{12}CHClF_2$ increases with increasing pressure.

The observed effects of experimental parameters on the IRMPD of $CHClF_2/Br_2$ mixtures suggest favorable conditions to large scale $^{13}$C separation. The absolute yield of $^{13}$C is largest in the $CHClF_2$ pressure range between 50–100 Torr. As the pressure of $Br_2$ is increased, the yield becomes larger. A beam from a $CO_2$ laser must be focused to some extent to induce IRMPD of $CHClF_2$ in large scale separation, because the parallel beam emerging from a laser cavity has usually a fluence below 2 J cm$^{-2}$. However, the fluence at a beam waist should not exceed 10 J cm$^{-2}$ to suppress the thermal chain leading to the formation of $CBrClF_2$. The change of the 9*P*(22) line into a line at its red side results in an increase in selectivity and a decrease in yield. On the other hand, a line at a blue side gives a lower selectivity and a higher yield, as compared to the 9*P*(22) line. Figure 15 shows typical infrared absorption spectrum of $CBr_2F_2$ enriched with $^{13}$C obtained under favorable experimental conditions to large scale $^{13}$C separation suggested from the above results. The $CBr_2F_2$ was isolated from the irradiated mixture by a preparative gas chromatograph equipped with a 3-m silica gel column (column temperature, 130°C). The $^{13}$C-atom fraction in $CBr_2F_2$ was determined to be 37% in mass spectrometric analysis. The spectrum for natural $CBr_2F_2$ has three intense bands with peaks at 830, 1090, and 1150 cm$^{-1}$ [19, 20]. In

addition to these peaks, the spectrum in Fig. 15 presents peaks at 800, 1060, and 1125 $cm^{-1}$ due to $^{13}CBr_2F_2$.

Finally, we attempted to produced $^{13}C$-enriched $CBr_2F_2$ using a larger pulse provided from a Lumonics 822 $CO_2$ TEA laser. The experimental conditions are: $CHClF_2$, 100 Torr; $Br_2$, 45 Torr; laser line, $9P(22)$; fluence at beam waist, 8 J $cm^2$; pulse number, 100 shots. $CBr_2F_2$ containing 47% $^{13}C$ was found to be produced at a rate of $1.9 \times 10^{-4}$ g $pulse^{-1}$. If the laser is operated at a repetition rate of 10 Hz, the production rate of $^{13}C$ amounts to 0.20 g $h^{-1}$. This value is close to the production rate of 0.22 g $h^{-1}$ for 50% $^{13}C$, which has been reported of the IRMPD of neat $CHClF_2$ using a 100-W laser (10 J, 10 Hz) [7].

## 3. Discussion

The experimental results obtained with the IRMPD of $CHClF_2/Br_2$ mixtures can be explained satisfactorily in terms of the following mechanism:

$$CHClF_2 + nhv \rightarrow CF_2 + HCl \quad (1)$$

$$CF_2 + HCl \rightarrow CHClF_2 \quad (2)$$

$$2CF_2 \rightarrow C_2F_4 \quad (3)$$

$$CF_2 + Br_2 \rightarrow CBr_2F_2^* \quad (4)$$

$$CBr_2F_2^* \rightarrow CBrF_2 + Br \quad (5)$$

$$CBr_2F_2^* + M \rightarrow CBr_2F_2 + M \quad (6)$$

$$CBrF_2 + Br_2 \rightarrow CBr_2F_2 + Br \quad (7)$$

$$2CBrF_2 \rightarrow C_2Br_2F_4 \quad (8)$$

$$2Br \rightarrow Br_2. \quad (9)$$

It has been well established in the product-analysis study [18] and in the direct mass-spectroscopic study using a molecular-beam technique [21] that the initial step in IRMPD of $CHClF_2$ is the decomposition of highly vibrationally excited $CHClF_2$ into a $CF_2$ radical and a HCl molecule. The threshold energy of the decomposition has been estimated to be 54 kcal $mol^{-1}$ [21].

We could not observe an appreciable amount of $CBrClF_2$ under the present experimental conditions, although the compound was found to be a main product in the IRMPD of the same mixture [22]. Since the laser line used in the previous study ($9R(36)$ at 1088 $cm^{-1}$) was much closer to the intense absorption peak due to $^{12}CHClF_2$, the absorption of large laser energy probably resulted in considerable temperature rise in the illuminated zone. The following thermal chain occurred and formed $CBrClF_2$.

$$Br + CHClF_2 \rightarrow HBr + CClF_2 \quad (10)$$

$$CClF_2 + Br_2 \rightarrow CBrClF_2 + Br. \quad (11)$$

We detected a large amount of $CBrClF_2$ in the irradiation of the mixture with the $9P(22)$ line, when the fluence was beyond 10 J $cm^{-2}$.

The Arrhenius parameters of reaction (2) reported previously are as follows: $\log A(cm^3\ mol^{-1}\ s^{-1}) = 11.35$, $E = 6.2$ kcal $mol^{-1}$ (1 kcal = 4.19 kJ) [23, 24]; $\log A = 11.33$, $E = 12.1 \pm 2.7$ kcal $mol^{-1}$ [23, 25]. Although the pre-exponential factors agree with each other, the activation energies show a large difference between them. From these parameters, the rate constants $k_2$ at 300 K are calculated to be $k_2 = 6.8 \times 10^6$ $cm^3\ mol^{-1}\ s^{-1}$ for $E = 6.2$ kcal $mol^{-1}$ and $k_2 = 3.3 \times 10^2$ $cm^3\ mol^{-1}\ s^{-1}$ for $E = 12.1$ kcal $mol^{-1}$. The rate constants of the dimerization reaction of $CF_2$ have been determined previously to be $k_{3D} = 1.3 \times 10^{11} (T/300\ K)^{1/2} \exp(-1200/RT)$ $cm^3\ mol^{-1}\ s^{-1}$ by Dalby [26] and $k_{3T} = (2.5 \pm 0.5) \times 10^6\ T^{1/2} \exp[-(200 \pm 50)/T]$ by Tyerman [27], where $k_{3D}$ corresponds to $2k_{3T}$ because of the difference in a definition. The rate constant at 300 K is figured out to be either $k_{3D} = 1.7 \times 10^{10}$ $cm^3\ mol^{-1}\ s^{-1}$ or $k_{3T} = 2.2 \times 10^{10}$ $cm^3\ mol^{-1}\ s^{-1}$. Therefore, the relative rate of the formation of $C_2F_4$ to that of $CHClF_2$ is expressed by the following equation.

$$\frac{R(C_2F_4)}{R(CHClF_2)} = \frac{k_3[CF_2][CF_2]}{k_2[CF_2][HCl]} = \frac{k_3[CF_2]}{k_2[HCl]} \geqq 2.5 \times 10^3 \frac{[CF_2]}{[HCl]}.$$

$[CF_2]$ may be in the same order as [HCl] in irradiated mixtures. Whether $E = 6.2$ kcal $mol^{-1}$ or $E = 12.1$ kcal $mol^{-1}$, $R(CHClF_2)$ is negligibly small as compared to $R(C_2F_4)$.

The rate constant of reaction 4 has been determined to be $k_4 = (1.6 \pm 0.5) \times 10^9$ $cm^3\ mol^{-1}\ s^{-1}$ at 550 K [28]. From the above-mentioned equations, $k_{3D} = 5.9 \times 10^{10}$ $cm^3\ mol^{-1}\ s^{-1}$ and $k_{3T} = 4.1 \times 10^{10}$ $cm^3\ mol^{-1}\ s^{-1}$ at 550 K. The ratio between the rates of reaction (3) and reaction (4) at 550 K can be given by the following equation.

$$\frac{R(C_2F_4)}{R(CF_2 + Br_2)} = \frac{k_3[CF_2][CF_2]}{k_4[CF_2][Br_2]} = (37 \text{ or } 51) \times \frac{[CF_2]}{[Br_2]}.$$

Under the present irradiation conditions, the temperature in the illuminated zone may be lower than 550 K because of the weak absorption of $CHClF_2$ for the $9P(22)$ line. The ratio of $[CF_2]$ to $[CHClF_2]$ is roughly estimated to be $0.7 \times 10^{-3}$ from the production yield per pulse and $V_{cell}/V_{ill}$ ($\sim 15$), where $V_{cell}$ and $V_{ill}$ are the volumes of the cell and the illuminated zone, respectively. Therefore, $CF_2$ radicals seem to be scavenged

mostly by $Br_2$, as $Br_2$ is larger than 10% of $CHClF_2$. However, we cannot estimate the ratio exactly at this moment, because the temperature in the illuminated zone and the activation energy of reaction (4) are unknown. In all the mixtures examined here, we could not find $C_2F_4$ as a product.

It is not clear what fraction of the excited $CBr_2F_2^*$ is stabilized via reaction (6). The exothermicity of reaction (4) has been estimated to be 67 kcal $mol^{-1}$ [22] or 51 kcal $mol^{-1}$ [29]. The dissociation energy of a C–Br bond is generally about 64 kcal $mol^{-1}$. However, the formation of $C_2Br_2F_4$ indicates the occurrence of reaction (5), since the compound is probably formed via the dimerization of $CBrF_2$ radicals. As the pressure of $Br_2$ is increased, the yield of $C_2Br_2F_4$ relative to that of $CBr_2F_2$ decreases rapidly owing to the competition between reactions (7) and (8) in addition to the competition between reactions (5) and (6).

At the beginning of the irradiation the $^{13}C$-atom fractions in $CBr_2F_2$ and $C_2Br_2F_4$ are close to each other, as shown in Fig. 3. However, the fraction in $C_2Br_2F_4$ becomes much larger than that in $CBr_2F_2$, as the pulse number is increased. This result was explained by the isotopically selective secondary decomposition of $CBr_2F_2$ in the previous paper [16]. The detailed examination on the pulse number effects on the product yields reveals that both $^{12}y(C_2Br_2F_4)$ and $^{13}y(C_2Br_2F_4)$ decrease much more rapidly with increasing pulse number as compared with $^{12}y(CBr_2F_2)$ and $^{13}y(CBr_2F_2)$. We attribute the rapid decreases to the secondary photochemical decomposition of $C_2Br_2F_4$ in this paper. Natural $C_2Br_2F_4$ in a liquid phase has an intense absorption band centered at 1007 $cm^{-1}$ [30]. Our measurement in a gas phase showed the absorption at 1015 $cm^{-1}$. The laser irradiation of this compound with the $9P(22)$ line at 1045.02 $cm^{-1}$ is likely to induce IRMPD via the absorption due to the band. Since the $9P(22)$ line is located at the blue side of the band peak, $^{12}C$-bearing molecules in $C_2Br_2F_4$ may be somewhat selectively decomposed in the secondary photolysis. As the result, $C_2Br_2F_4$ is further enriched with $^{13}C$. The mechanism is considered to be:

$$C_2Br_2F_4 + n'h\nu \rightarrow C_2BrF_4 + Br \quad (12)$$

$$\rightarrow 2\,CBrF_2 \quad (13)$$

$$C_2BrF_4 + Br_2 \rightarrow C_2Br_2F_4 + Br. \quad (14)$$

The path via reaction (13) followed by reaction (7) contributes the net decomposition of $C_2Br_2F_4$ in the presence of $Br_2$.

The first-stage IRMPD is intended to produce more or less 40% $^{13}CBr_2F_2$ at a yield as large as possible. The further enrichment must be made at the second stage. Figure 15 shows that $^{12}CBr_2F_2$ and $^{13}CBr_2F_2$ have the sharp peaks at 1090 and 1060 $cm^{-1}$, respectively, in their infrared spectra. Ritter has demonstrated isotopically selective decomposition and isotopic segregation in the IRMPD of natural $CBr_2F_2$ [31]. Since a $CO_2$ laser was tuned to the line at 1081 $cm^{-1}$ in their study, $^{12}C$-bearing molecules selectively decomposed and unconsumed $CBr_2F_2$ showed $^{12}C$-depletion as compared to natural carbon. On the other hand, our previous results have demonstrated that $^{13}C$-bearing molecules decompose preferentially in the irradiation of $CBr_2F_2$ with the $9P(28)$ line at 1039.37 $cm^{-1}$ [16]. In the presence of $O_2$, we finally obtained $CF_2O$ at a $^{13}C$-atom fraction as high as 86%, using $CBr_2F_2$ at about 30% as a starting material. The mechanism leading to the formation of $CF_2O$ may be essentially the same as the IRMPD of $CCl_2F_2/O_2$ mixtures [32, 33].

$$CBr_2F_2 + n''h\nu \rightarrow CBrF_2 + Br \quad (15)$$

$$CBrF_2 + O_2 \rightarrow CF_2O + BrO \quad (16)$$

$$2\,BrO \rightarrow Br_2 + O_2. \quad (17)$$

One can easily convert the $CF_2O$ into $CO_2$ without a change in $^{13}C$ concentration via hydrolysis:

$$CF_2O + H_2O \rightarrow CO_2 + 2\,HF. \quad (18)$$

The IRMPD of $CBr_2F_2/O_2$ mixtures must be studied in details to optimize the experimental conditions for the second-stage enrichment.

## References


1. V.S. Letokhov: *Nonlinear Laser Chemistry* (Springer, Berlin, Heidelberg 1983) p. 252
2. W. Fuss, W.E. Schmid: Ber. Bunsenges. Phys. Chem. **83**, 1148 (1979)
3. M. Gauthier, C.G. Cureton, P.A. Hackett, C. Willis: Appl. Phys. B **28**, 43 (1982)
4. G.I. Abdushelishvili, O.N. Avatkov, V.N. Bagratashvili, V.Yu. Baranov, A.B. Bakhtadze, E.P. Velikhov, V.M. Vetsko, I.G. Gverdtsitelii, V.S. Dolzhikov, G.G. Esadze, S.A. Kazakov, Yu.R. Kolomiiski, V.S. Letokhov, S.V. Pigul'skii, V.D. Pis'mennyi, E.A. Ryabov, G.I. Tkeshelashvili: Sov. J. Quant. Electron. **12**, 459 (1982)
5. H. Kojima, T. Fukumi, S. Nakajima, Y. Maruyama, K. Kosasa: Appl. Phys. B **30**, 143 (1983)
6. M. Gauthier, A. Outhouse, Y. Ishikawa, K.O. Kutschke, P.A. Hackett: Appl. Phys. B **35**, 173 (1984)
7. A. Outhouse, P. Lawrence, M. Gauthier, P.A. Hackett: Appl. Phys. B **36**, 63 (1985)
8. V.Yu. Baranov: IEEE J. QE-**19**, 1577 (1983)
9. A.V. Evseev, V.S. Letokhov, A.A. Puretzky: Appl. Phys. B **36**, 93 (1985)
10. M. Drouin, M. Gauthier, R. Pilon, P.A. Hackett, C. Willis: Chem. Phys. Lett. **60**, 16 (1978)
11. T. Watanabe, T. Oyama, O. Hayashi, Y. Ishikawa, T. Ishii, S. Arai: Nippon Kagaku Kaishi, 1517 (1984)

12. S. Bittenson, P.L. Houston: J. Chem. Phys. **67**, 4819 (1977)
13. H. Kojima, T. Fukumi, S. Nakajima, Y. Maruyama, K. Kosasa: Chem. Phys. Lett. **95**, 614 (1983)
14. S. Arai, T. Watanabe, Y. Ishikawa, T. Oyama, O. Hayashi, T. Ishii: Chem. Phys. Lett. **112**, 224 (1984)
15. P. Ma, K. Sugita, S. Arai: Chem. Phys. Lett. **137**, 590 (1987)
16. S. Arai, K. Sugita, P. Ma, Y. Ishikawa, H. Kaetsu, S. Isomura: Chem. Phys. Lett. **151**, 516 (1988)
17. J.G. McLaughlin, M. Poliakoff, J.J. Turner: J. Mol. Struc. **82**, 51 (1982)
18. E. Grunwald, K.J. Olszyna, D.F. Dever, B. Knishkowy: J. Am. Chem. Soc. **99**, 6515 (1977)
19. C.E. Decker, F.F. Cleveland, R.B. Bernstein: J. Chem. Phys. **21**, 189 (1953)
20. C.E. Decker, A.G. Meister, F.F. Cleveland, R.B. Bernstein: J. Chem. Phys. **21**, 1781 (1953)
21. Aa.S. Sudbø, P.A. Schulz, Y.R. Shen, Y.T. Lee: J. Chem. Phys. **69**, 2312 (1978)
22. S. Popok, C.M. Lonzetta, E. Grunwald: J. Org. Chem. **44**, 2377 (1979)
23. D.S.Y. Hsu, M.E. Umstead, M.C. Lin: ACS Symp. Ser. **66**, 128 (1978)
24. J.W. Edwards, P.A. Small: Nature **4939**, 1329, June 27, 1964
25. G.R. Barnes, R.A. Cox, R.F. Simmons: J. Chem. Soc. (B) 1176 (1971)
26. F.W. Dalby: J. Chem. Phys. **41**, 2297 (1964)
27. W.J.R. Tyerman: Trans. Faraday Soc. **65**, 1188 (1969)
28. K. Sugawara, T. Nakanaga, H. Takeo, C. Matsumura: Chem. Phys. Lett. **134**, 347 (1987)
29. J.C. Stephenson, D.S. King: J. Chem. Phys. **69**, 1485 (1978)
30. R.E. Kagarise, L.W. Daasch: J. Chem. Phys. **23**, 130 (1955)
31. J.J. Ritter: J. Am. Chem. Soc. **100**, 2441 (1978)
32. J.J. Ritter, S.M. Freund: J.C.S. Chem. Commun. 811 (1976)
33. W.S. Nip, P.A. Hackett, C. Willis: Can. J. Chem. **59**, 2703 (1981)